

## Structural and optical characterisation of thermally evaporated tungsten trioxide (WO<sub>3</sub>) thin films

M.G. HUTCHINS<sup>A</sup>, O. ABU-ALKHAIR<sup>B,\*</sup>, M.M. EL-NAHASS<sup>C</sup> and K. ABD EL-HADY<sup>D</sup>

(a) School of Engineering, Oxford Brookes University, England

(b) Physics Department, Faculty of Science, King Abdulaziz University, Jeddah, Saudi Arabia

(c) Physics Department, Faculty of Education, Ain Shams University, Cairo, Egypt,

(d) Physics Department, Faculty of Science, Minia University, Menia, Egypt

\*Corresponding author. E-mail address: oabukhar@kaau.edu.sa

**ABSTRACT.** Thin films of amorphous tungsten trioxide (WO<sub>3</sub>) have been thermally evaporated onto quartz substrates held at 350K. Annealing at 725K caused the formation of crystalline WO<sub>3</sub>. XRD analysis revealed monoclinic structure with lattice parameters of  $a=7.311\pm 0.05$  Å,  $b=7.603\pm 0.05$  Å,  $c=7.713\pm 0.05$  Å and  $\beta=91.137^\circ$ . Optical properties were investigated for both the amorphous and annealed films by using spectrophotometric measurement of transmittance and reflectance at normal incidence in the wavelength range of 200-2500 nm. The obtained spectra showed that all the films are transparent above  $\lambda=500$  nm and the measured optical constants are independent of the film thickness. Both the refractive index,  $n$ , and absorption index,  $k$ , were determined for the amorphous and crystalline films. The optical dispersion parameters have been analysed by single oscillator model. The values of  $E_0$  and  $E_d$  were found to be 5.86, 14.43 eV for the amorphous films and 2.96, 11.30 eV for the crystalline films. Indirect optical transitions with corresponding energy gaps = 3.28 and 3.03 eV for amorphous and crystalline films, respectively, were obtained. The obtained results are compared and discussed.

**Keyword:** Thin films, Tungsten trioxide, Optical constants

### 1. Introduction

Transition metal oxides constitute a very interesting class of materials because of the various properties that they exhibit. Among the thin films of transition metal oxides, tungsten trioxide (WO<sub>3</sub>) has received increasing attention because of their electrochromic properties in the visible and infrared. Their optical properties can be switched reversibly under certain electrochemical conditions (Smith, 1982). During the last several decades, many materials have been examined with respect to their use in switchable windows (Lampert *et al.* 1989, Agrawal *et al.* 1993, Akl *et al.* 2003). WO<sub>3</sub> still seems to be among

the best inorganic electrochromic material due to its high coloration efficiency and relatively low price. The electrochromic materials can be switched from transparent to coloured state by using an external voltage and a proton source. In this way, the change of state can be described by a simultaneous injection and extraction of the electrons and protons (Lampert *et al.* 1989, Agrawal *et al.* 1993). This phenomenon is applied in electrochromic, optochromic and thermo-chromic devices, such as energy saving windows (smart windows), solar roofing, anti glare rear-view mirrors and gases sensors (Hoei *et al.* 2000).

In polycrystalline films, the injected electrons behave as free-carriers leading to an increase in near infrared (NIR) reflectivity (Goldner *et al.* 1986, Kamal *et al.* 2004). Nevertheless, scattering of the excess free electrons by extended defects, leads to lower reflectivity in this region (Goldner *et al.*, 1984). The characteristics of  $\text{WO}_3$  films depend strongly on the condition of film preparation. Different techniques used for  $\text{WO}_3$  films preparation such as, thermal and electron beam evaporation (Agrawal *et al.*, 1993), RF sputtering, chemical vapour deposition (CVD), anodic oxidation, sol-gel (Ozkan *et al.*, 2001), spray pyrolysis (Regragui *et al.*, 2003) and magnetron sputtering (Akl *et al.* 2003, Kamal *et al.* 2004) are used.

In this work, amorphous tungsten oxide films have been prepared by thermal evaporation. The changes in the structural and optical properties of the as deposited and annealed films as a function of film thickness in the amorphous and polycrystalline were investigated. The structural and morphological changes due to annealing are studied. The optical properties for both types of films have been investigated.

## 2. Experimental procedure

Tungsten trioxide ( $\text{WO}_3$ ) powder used in this study was obtained from BDH chemical Ltd Co., with purity of 99.986%. Thin films of different thicknesses were deposited by vacuum thermal evaporation method, using a high vacuum coating unit (Edwards, E306A). The films were deposited onto pre-cleaned glass (for structural investigation) and optically flat quartz substrates (for optical investigation) maintained at 350 K. Thin films were deposited from a molybdenum evaporator charged by  $\text{WO}_3$  in a vacuum of  $10^{-5}$  Pa. The deposition rate was controlled at  $1\text{nm s}^{-1}$  using a quartz crystal thickness monitor (FTM6, Edwards). The film thickness ranged between 100 nm and 300 nm. Thickness of the film is determined by Tolansky's technique (Tolansky, 1988). The films were then annealed at 723 K for 2 hour in air.

The structural properties of powder and thin films were studied using X-ray diffraction technique. A Philips X-ray diffractometer (model X'pert) was used for the measurements, which utilized monochromatic  $\text{CuK}_\alpha$  radiation operated at 40kV and 25mA. The diffraction patterns were recorded automatically with a scanning speed of 0.05 degrees per minute.

Optical properties were investigated for both the as deposited and annealed films by spectrophotometric measurement of transmittance,  $T$ , and reflectance,  $R$ , at normal incidence in the wavelength range of 200-2500 nm using a double beam spectrophotometer (JASCO model V570-UV-VIS-NIR).

The  $T(\lambda)$  and  $R(\lambda)$  were calculated according to the relations (Agiev *et al.* 1978, Shklyarevskii *et al.* 1969).

$$T(\lambda) = (I_t/I_q)(1-R_q) \quad (1)$$

and

$$R(\lambda) = (I_{tr}/I_{Ar})R_{Al}[1+(1-R_q)^2]-TR_q \quad (2)$$

where  $I_t$  and  $I_q$  are the intensities of light passing through film-quartz system and reference quartz substrate respectively.  $I_{tr}$  and  $I_{Ar}$  are the intensities of light reflected from the sample and that from the reference mirror, respectively, and  $R_q$  is the reflectance of quartz. The refractive index,  $n$ , and the absorption index,  $k$ , were computed by a modified version (El-Nshass *et al.*, 1988) of Abélés technique (Abeles & Theye, 1966) based on solving the two non-linear equation:

$$f_i(n,k) = T_{n,k} - T_{exp} = 0 \quad (3)$$

$$f_r(n,k) = R_{n,k} - R_{exp} = 0 \quad (4)$$

where  $T_{n,k}$  and  $R_{n,k}$  refer to Murmann's exact equations (Heavens, 1965). The experimental errors were taken into account as  $\pm 5\%$  for the film thickness measurements and  $\pm 1\%$  for  $T$  and  $R$ . Calculations revealed error of  $\pm 5\%$  for the refractive and 3% for the absorption index.

### 3. Results and discussion

#### 3.1. Structural properties

X-ray diffraction (XRD) patterns obtained from powder and thin film forms of tungsten trioxide ( $WO_3$ ) are shown in Fig 1. It shows that the X-ray diffraction pattern of the as-deposited films is amorphous in nature and it exhibits a broad peak around  $2\theta = 23^\circ$ . The effect of annealing on the structure of the  $WO_3$  film is, also, shown in Fig. 1. When the amorphous film was annealed at 723 K 2h, the X-ray diffraction pattern exhibited a new diffraction pattern with four peaks, which was identified primarily as polycrystalline monoclinic  $WO_3$  phase with reference to the powder diffraction pattern. It can be noted that the pattern for both powder and thin film show polycrystalline form. Indexing was carried out for the patterns and their peaks were identified as monoclinic crystal system with lattice constants of  $a = 7.311 \pm 0.05 \text{ \AA}$ ,  $b = 7.603 \pm 0.05 \text{ \AA}$ ,  $c = 7.713 \pm 0.05 \text{ \AA}$  and  $\beta = 91.137^\circ$  (ICDD Card No.83-0951 for  $WO_3$ ).

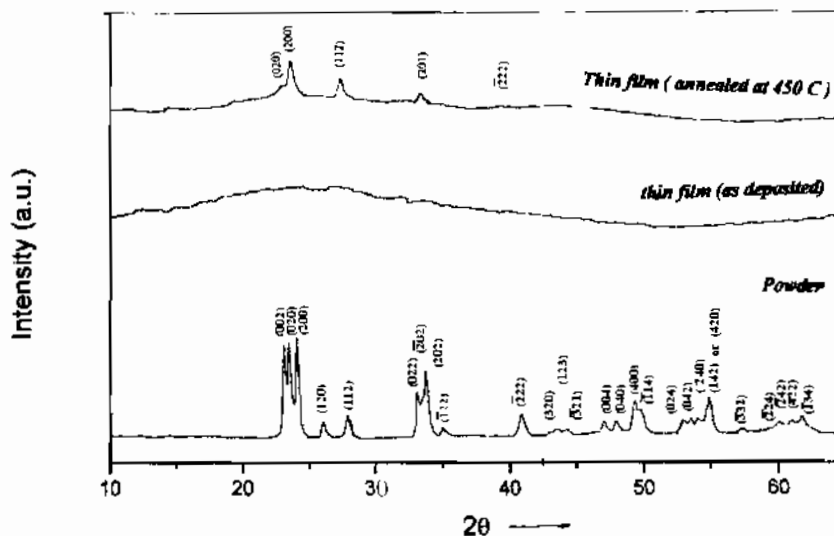


Fig. 1. X-ray diffraction pattern of  $WO_3$  in powder and thin film forms.

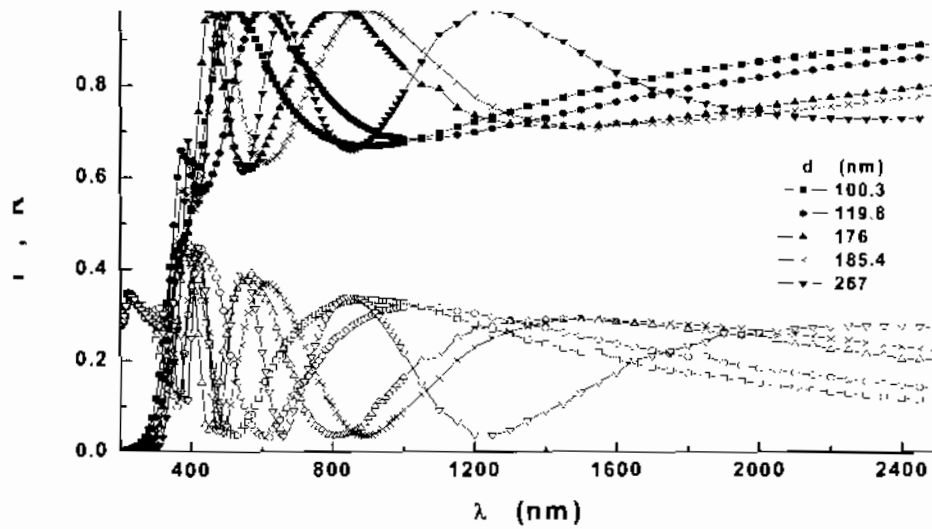


Fig. 2. Spectral distribution of normal incidence transmittance,  $T$ , and reflectance,  $R$ , for amorphous  $\text{WO}_3$  films with different thicknesses.

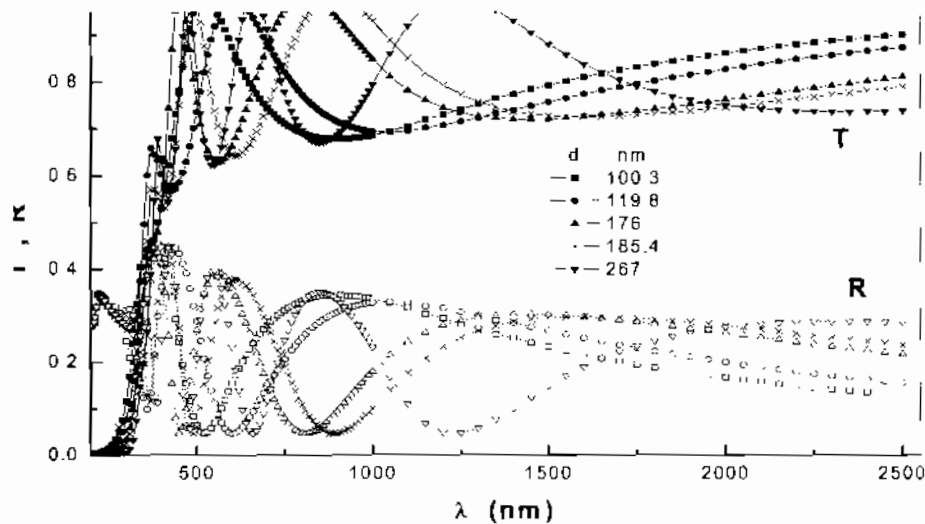


Fig. 3. Spectral distribution of normal incidence transmittance,  $T$ , and reflectance,  $R$ , for Crystalline  $\text{WO}_3$  films with different thicknesses.

### 3.2. Optical properties

Figs. 2 and 3 show the spectral transmittance and reflectance for as-deposited films at different thicknesses and for the same films annealed at 723 K for 2h, in the wavelength range 200-2500 nm, respectively. As a general observation, it can be noted that beyond the absorption edge,  $\lambda > 500$  nm,  $T + R = 1$  which implies that all films become transparent and no light is scattered or absorbed. The optical constants (real and imaginary parts of the complex refractive index) were determined from the absolute values of transmittance and reflectance of films by exact formulas (Heavens, 1965).

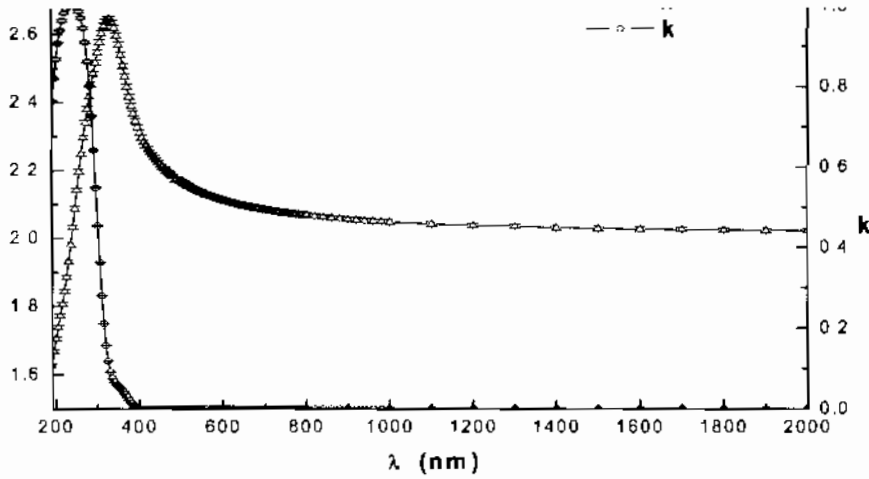
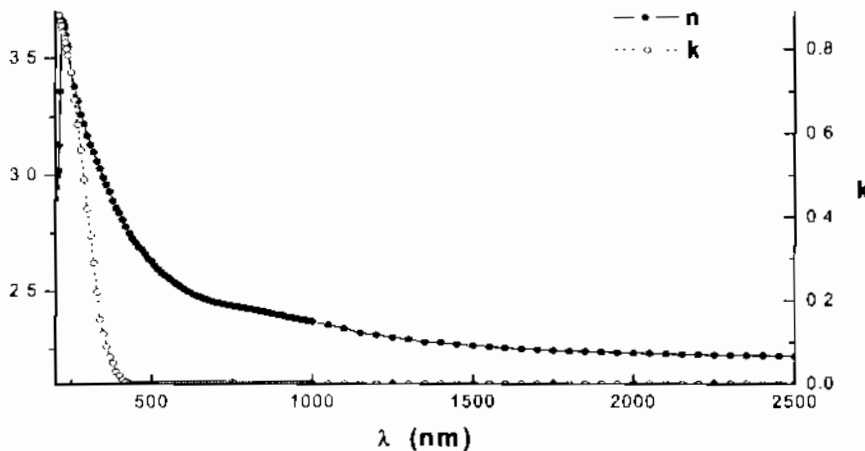
Fig. 4. Spectral behaviour of both  $n$  and  $k$  for amorphous  $\text{WO}_3$  filmsFig. 5. Spectral behaviour of both  $n$  and  $k$  for crystalline  $\text{WO}_3$  films

Fig. 4 and Fig. 5 show the spectral behaviour of both the refractive index,  $n$ , and the absorption index,  $k$ , in the wavelength range 200–2500 nm for the amorphous and crystalline films, respectively, they represent the average values of both  $n$  and  $k$  for the investigated thickness range 100–267 nm as a function of wavelength. The calculated standard deviation was found to be within the calculated experimental error indicating that the optical constants are independent of the film thickness for the all studied films. It is clear that the peak value of  $n$  observed for amorphous films disappear upon annealing, which reflects structural changes as confirmed by X-ray study. Both curves show normal dispersion beyond  $\lambda = 500$  nm.

The dispersion of refractive index,  $n$ , in  $\text{WO}_3$  films was analysed using the concept of the single oscillator and can be expressed by the Wemple and DiDomenico relationship (Wemple & DiDomenico, 1971) as

$$n^2 - 1 = E_d E_0 / [ E_0^2 - E^2 ] \quad (5)$$

where  $E$  is the photon energy,  $E_0$  is the oscillator energy and  $E_d$  is the dispersion energy. The parameter  $E_d$ , which is a measure of the intensity of the inter-band optical transition, does not depend significantly on the band gap. A plot of  $(n^2 - 1)^{-1}$  versus  $E^2$  of amorphous and crystalline films is illustrated in Fig. 6 (a & b). The values of  $E_d$  and  $E_0$  were obtained

from the slope and the intercept resulting from the extrapolation of the lines as 14.43, 5.86 eV and 11.30, 2.96 eV, respectively, for the amorphous and crystalline films. As observed

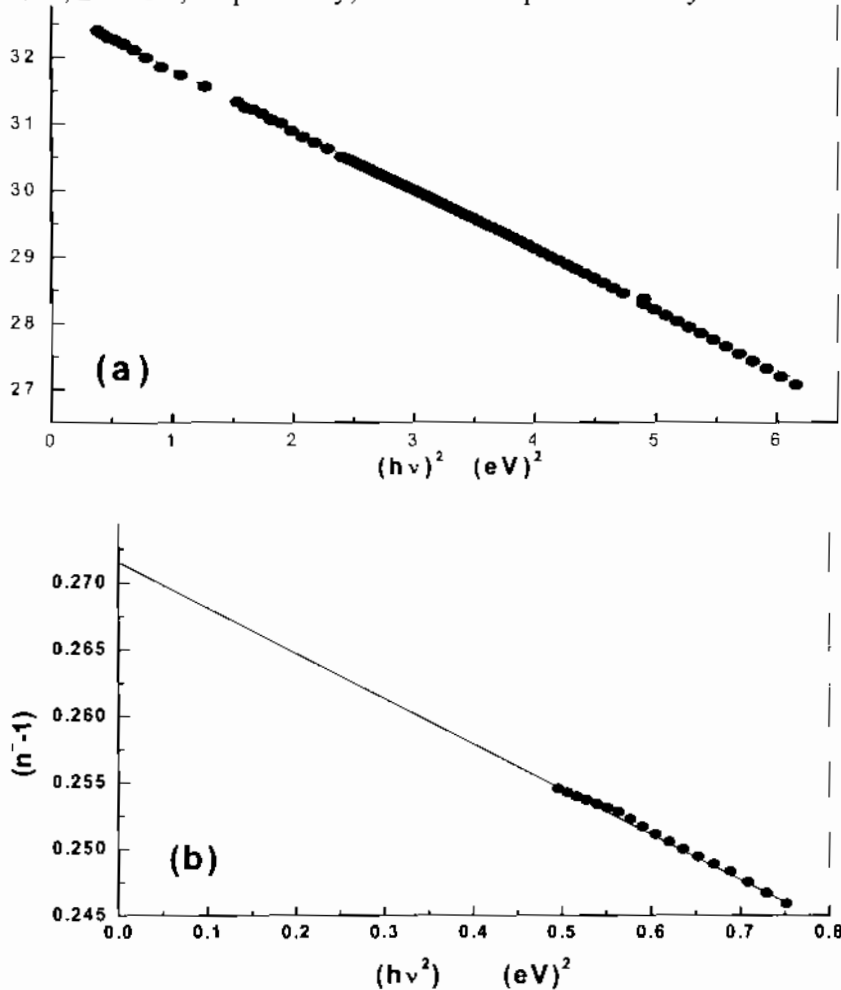


Fig. 6. A plot of  $(n^2 - 1)^{-1}$  versus  $E^2$  of (a) amorphous and (b) crystalline films

there is a little effect of annealing on the oscillating and dispersion energies. The optical dielectric constant ( $\epsilon_\infty = n_\infty^2$ ) was calculated as 4.72 and 3.52 for amorphous and crystalline films, respectively. A simple connection between the single oscillator parameters  $E_0$  and  $E_d$  and the imaginary part of the dielectric constant  $\epsilon_2(\nu)$  spectrum can be expressed in terms of the  $r$ th moments of the  $\epsilon_2(\nu)$  as (Wemple & DiDomenico, 1971)

$$E_0^2 = M_{-1} / M_{-3} \quad (6)$$

and

$$E_d^2 = M_{-1}^3 / M_{-3} \quad (7)$$

The oscillator energy  $E_0$  is independent of the scale of  $\epsilon_2$ . The values of  $M_{-1}$  and  $M_{-3}$  are 3.03 and 2.46 eV<sup>-2</sup>, respectively, for the amorphous films and 0.09 and 0.07 eV<sup>-2</sup>, respectively, for the crystalline films.

The relation between the lattice dielectric constant,  $\epsilon_L$ , wavelength,  $\lambda$ , and refractive index,  $n$ , is given by the relation (Robert *et al.* 1985)

$$n^2 = \epsilon_L - e^2 / \pi c^2 (N / m^3) \lambda^2 \quad (8)$$

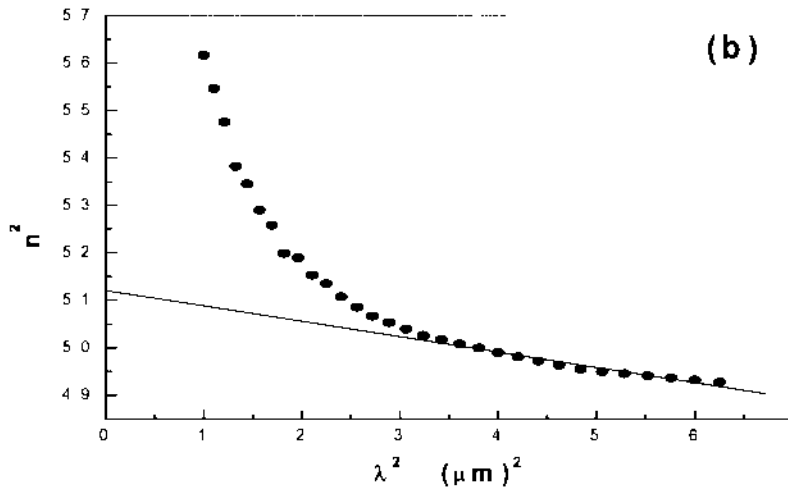
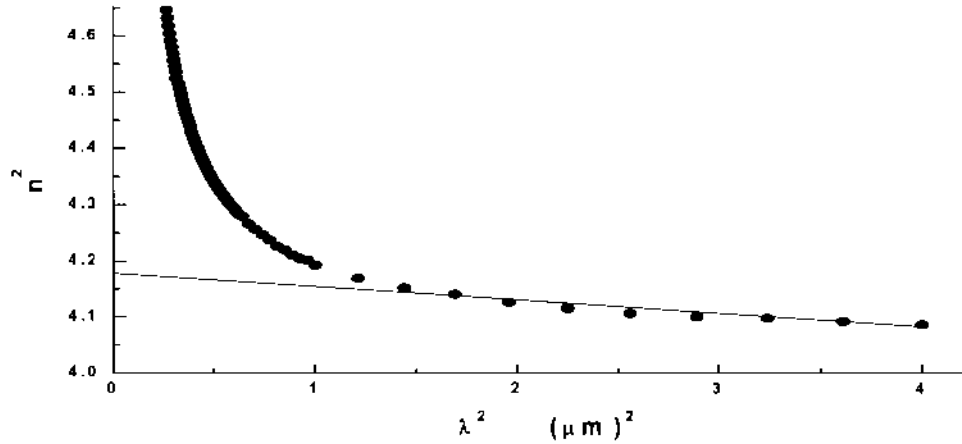


Fig. 7. Variation of  $n^2$  versus  $\lambda^2$  for (a) amorphous and (b) crystalline films.

Where  $\epsilon_L$  is the lattice dielectric constant and  $N/m^*$  is the ratio of carrier concentration to the effective mass. The  $n^2$  versus  $\lambda^2$  plot shown in Fig. 7 (a & b) is linear at higher wavelengths verifying equation (8). The values of  $\epsilon_L$  and  $(N/m^*)$  were determined from the extrapolation of these plots to  $\lambda^2 = 0$  and from the slopes of the graph. The obtained values are 4.18 and  $1.40639 \times 10^{46} \text{ gm}^{-1}\text{cm}^{-3}$  respectively for the amorphous films and 5.125 and  $2.27444 \times 10^{47} \text{ gm}^{-1}\text{cm}^{-3}$ , respectively, for the crystalline films. The disagreement between the values of  $\epsilon_\infty$  and  $\epsilon_L$  may be due to free carrier contribution.

In order to study the type of optical transitions as well as the value of the energy gap, the Bardeen equation was used in the following form (Bardeen *et al.* 1965)

$$(\alpha h\nu)^r = A (h\nu - E_g) \quad (9)$$

Where  $A$  is a parameter that depends on the transition probability,  $E_g$  is the energy band gap and  $r$  is a number which characterizes the transition process, where  $r=2$  and  $r=2/3$  for direct allowed and forbidden transitions, respectively and  $r=1/2$  and  $1/3$  for indirect allowed and forbidden transitions, respectively. The plot of  $(\alpha h\nu)^{1/2}$  versus  $h\nu$  give a straight line over a range above the absorption edge as shown in Fig. 8a for the amorphous and Fig. 8b for polycrystalline films. The weak absorption is assumed to be due to indirect transition involving participation of phonons in the process. A phonon is either emitted or

absorbed, depending on whether the energy of the phonon is more than the indirect band gap or less. The phonon associated with the transition process might be attributed to the stretching band of  $\text{WO}_3$  having energy of 3.27 and 3.45 eV respectively for the amorphous and crystalline  $\text{WO}_3$  films.

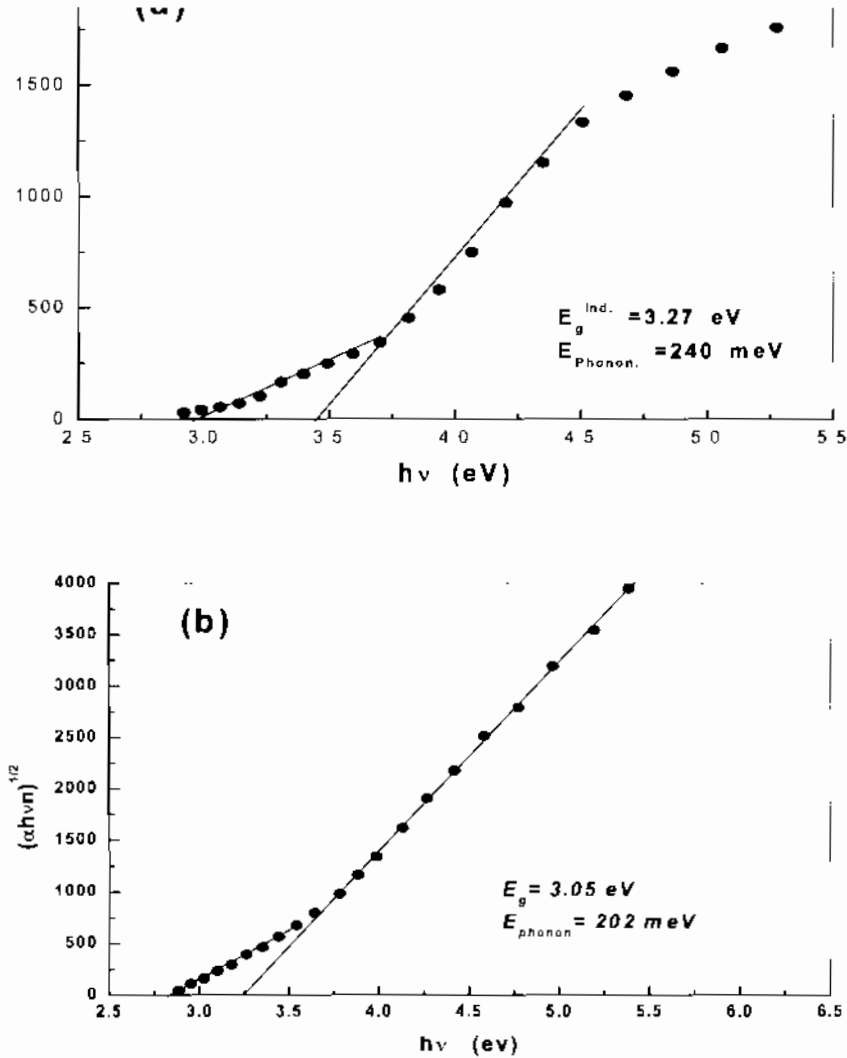


Fig. 8. Plot of  $(\alpha h\nu)^{1/2}$  versus  $(h\nu)$  for (a) amorphous and (b) crystalline films

#### 4. Conclusions

Amorphous tungsten oxide thin films have been thermally evaporated under vacuum of  $\sim 10^{-5}$  Pa. The X-ray study shows that transformation of the amorphous to crystalline occurs at an annealing temperature of 725 K. Formation of the monoclinic phase of lattice constants of  $a=7.311\pm 0.05$  Å,  $b=7.603\pm 0.05$  Å,  $c=7.713\pm 0.05$  Å and  $\beta=91.137^\circ$ . Calculation of the optical constants showed that both types of film pass normal dispersion beyond  $\lambda=500$  nm. Analyses of the absorption part revealed an indirect gap for amorphous films.



## References

- Agrawal, A., Cronin, J.P. and Zhung, R. *Sol. Energy Mater.* **31**, (1993) 9.
- Hoei, A., Kish, L.B., Vajtai, R., Niklasson, G.A., Grangvist, C.G. and Olsson, E. *Mater. Res. Soci. Symp. Proc.* **581**, (2000) 15.
- Akl, A.A., Kamal, H. and Abdel-Hady, K., *Physica*, **B 325**, (2003) 65–75.
- Lampert, C.M. and Grangvist, C.G. (Eds.), “*Large area chromogenics materials and devices or transmittance control*”. SPIE S4, Optical Engineering Press, Bellingham, USA 1989.
- Özkan, E. and Tepehan, F.Z. *Solar Energy Materials and Solar cells*, **68**, (2001) 265.
- Abélés, F. and Theye, M.L. *Surf. Sci.*, **5**, (1966) 325.
- Kamal, H., Akl, A.A. and Abdel-Hady, K. *Physica*, **B 349**, (2004) 192–205.
- Shklyarevskii, I.N., Kornveeva, T.I. and Zozula, K.N. *Opt. Spect.*, **27**, (1969) 174.
- Bardeen, J., Slatt, F.J. and Hall, L. *Photoconductivity Conf.*, **146**, Wiley, New York, (1965).
- Robert, J., Mark, A. and Alexander, W. *J. Appl. Optics*, **24**, (1985) 22.
- Agiev, L.A. and Shklyarevskii, I.N. *J. Prekel Spekt.*, **76**, (1978) 380.
- Regragni, M., Addou, M., Outzourhit, A., Elb. El-Idrissi, Kachouane, A. and Bongriue, A. *Solar Energy Materials and Solar cells*, **77**, (2003) 341.
- El-Nahass, M.M., Soliman, H.S., El-Kadry, N., Morsy, A.Y. and Yaghamour, S. *J. Mater. Sci. Lett.*, **7**, (1988) 325.
- Heavens, O.S. “*Optical Properties of Thin Solid Films*”, Dover Publication, New York, (1965) 55.
- Goldner, R.B., Brofos, A., Foley, G., Goldner, E.L., Hass, T., Henderson, W., Norton, P., Ratnam, B.A., Weis, N. and Wong, K.K. *SPIE Proc.*, **502**, (1984) 64.
- Goldner, R.B., Chapman, R.L., Foley, G., Goldner, E.L., Hass, T., Norton, P., Seward, G. and Wong, K.K. *Sol. Energy Mater.*, **14**, (1986) 195.
- Tolansky, S. “*Multiple beam interferometry of surface and films*”, Oxford University press, (1988) 147.
- Wemple, S.H. and DiDomenico, M. *Phys. Rev.*, **B 3**, (1971) 1338.
- Dautromt Smith, W.C. *Disply*, **3**, (1982)67.

## الخصائص التركيبية والضوئية لأفلام رقيقة من أكسيد التانجستين الثلاثي (WO<sub>3</sub>) المحضرة بطريقة التبخير الحراري

م. هتشنز<sup>(١)</sup>، ع. أبو الخير<sup>(٢)</sup>، م. النحاس<sup>(٣)</sup> و ك. عبدالهادي<sup>(٤)</sup>

<sup>(١)</sup> مختبر أبحاث مواد الطاقة الشمسية، كلية الهندسة، جامعة أكسفورد بروكس - المملكة المتحدة

<sup>(٢)</sup> قسم الفيزياء، كلية العلوم، جامعة الملك عبدالعزيز، جدة - المملكة العربية السعودية

<sup>(٣)</sup> قسم الفيزياء، كلية التربية، جامعة عين الشمس، القاهرة - جمهورية مصر العربية

<sup>(٤)</sup> قسم الفيزياء، كلية العلوم، جامعة المنيا، المنيا - جمهورية مصر العربية

المستخلص. حضرت أفلام من أكسيد التنجستن الثلاثي بتقنية التبخير الحراري على شرائح من الزجاج المبلور (كوارتز) عند درجات حرارة ٨٠ الى ٢٥٠ درجة مئوية. وتم تليدين الأفلام عند درجة حرارة ٤٥٠؛ درجة مئوية مما أدى إلى تحولها من الحالة الأمورفية إلى المتبلورة وتحليل نتائج الأفلام المتبلورة بتقنية حيود الأشعة السينية (XRD) اتضح تبلور المركب في نظام احادي الميل بثوابت شبكية

$$a = 7.311 \pm 0.05, b = 7.603 \pm 0.05, c = 7.713 \pm 0.05, \beta = 91.137^\circ$$

درست الخواص الضوئية للأفلام كما رسبت وبعد تليدينها باستخدام جهاز الطيف الضوئي (Spectrophotometer) من خلال قياس الانعكاسية والنفاذية للأطوال الموجية للمدى ما بين ٢٠٠-٢٥٠٠ نانومتر وحدد معامل الامتصاص k ومعامل الانكسار n لحالتي الأفلام.

تم تحليل عوامل التثنت الضوئية باستخدام نموذج المتذبذب الأحادي وحددت طاقة التذبذب E<sub>0</sub> وطاقة التثنت E<sub>g</sub> المطورة بطريقة ويميل وداي دومينكو وقيمتها ١٤,٤٣-٥,٨٦ إلكترون فولت للأفلام الأمورفية و ٢,٩٦-١١,٩٨ إلكترون فولت للأفلام المتبلورة على التوالي. وحسبت فجوة الطاقة غير المباشرة E<sub>g</sub> لكلي الحالتين وكانت ٣,٢٢ إلكترون فولت للأفلام الأمورفية و ٢,٢٨ إلكترون فولت للأفلام المتبلورة.

وتمت مقارنة النتائج مع النتائج المنشورة وشرحت.